International Journal of Microstructure and Materials Properties

ISSN online: 1741-8429 - ISSN print: 1741-8410
https://www.inderscience.com/ijmmp

An experimental study on mechanical properties of UV cured 3D nanofibre printing materials

Hai Long, Shanjun Long

DOI: 10.1504/IJMMP.2024.10061242

Article History:

Received:	29 April 2023
Last revised:	02 June 2023
Accepted:	14 July 2023
Published online:	05 January 2024

An experimental study on mechanical properties of UV cured 3D nanofibre printing materials

Hai Long

School of Design and Art,
Changsha University of Science and Technology,
Changsha, 410114, China
Email: longhai777@163.com

Shanjun Long*

The 23rd Metallurgical Construction Group Co., Ltd. of Minmetals,
Changsha, 410116, China
Email: Longshanj@163.com
*Corresponding author

Abstract: To improve the mechanical properties of UV cured 3D printing materials after curing, this paper proposes a study on the mechanical properties of UV cured 3D nanofibre printing materials. The THBP modified nano TiO_2 is prepared as a subsequent auxiliary material, epoxy acrylate (EA) as a prepolymer, dipropylene glycol diacrylate (DPGDA) as a monomer, and phenyl bis (lithium phenyl-2,4,6-trimethylbenzoylphosphinate) phosphine oxide as a photoinitiator. A UV curable 3D printing material was prepared by adding THBP modified nano TiO_2 in different proportions, and analysing the mechanical properties of the materials prepared. THBP modified nano TiO_2 with different proportions of self synthesised THBP was added in order to achieve the research of strengthening and toughening modification and to improve its mechanical properties. The experimental results show that when the content of TEBP-TiO_2 is 5 wt%, the tensile strength and impact strength of the samples prepared after UV curing reach the maximum value of 51.3 MPa and 22.1 KJ/m^2, respectively. With the gradual increase of the content of THBP-TiO_2, the initial decomposition temperature and the maximum decomposition temperature of the materials increase. The residual mass of thermal decomposition is increased and the thermal stability is improved.

Keywords: UV curing; 3D printing; mechanical properties; nanofibres; THBP modification.

Reference to this paper should be made as follows: Long, H. and Long, S. (2024) 'An experimental study on mechanical properties of UV cured 3D nanofibre printing materials', *Int. J. Microstructure and Materials Properties*, Vol. 17, No. 1, pp.32–48.

Biographical notes: Hai Long graduated from the Changsha University of Science and Technology in Electrical Engineering and Automation, and currently a senior experimenter in the Experimental Center of School of Design and Art, Changsha University of Science and Technology. His main research directions involve the development and innovation of digital media art, the digital dissemination and promotion of Huxiang culture.

Shanjun Long is majoring in Marketing and Planning at the Beijing University of Civil Engineering and Architecture and currently a senior marketing manager of the Department of Investment Business of the 23rd Metallurgical Construction Group Co., Ltd. of Minmetals. His main research direction involves investment and financing platform system solution services.

1 Introduction

In traditional material reduction processing methods, it is usually necessary to use cutting, drilling, and other methods to process raw materials, which requires significant reduction and treatment of raw materials, resulting in a large amount of material waste. Unlike traditional methods, 3D printing technology revolves around the basic core of 'discretisation stacking'. When using this method to manufacture products, a 3D model of the piece to be printed is generated through computer-aided generation, and materials are added layer by layer (Liu et al., 2022) to minimise waste of raw materials and utilise digital model files to use adhesive or polymerisable materials, Fine printing is carried out according to the pre designed path, and the final layer upon layer of printed materials are used to construct the designed physical components, resulting in higher accuracy and quality of the product (Yong et al., 2022). Due to the advantages of rapid prototyping, low cost, and reduced human participation, this technology has been widely used (Gzab et al., 2022), such as medical, industrial design, aerospace and other fields (Gzab et al., 2022). In the future, with the continuous emergence of new materials, designs, and technologies, 3D printing technology will continue to innovate and develop, bringing more convenience and surprises to people.

The UV curing 3D printing is the combination of additive manufacturing and rapid prototyping technology. Compared with the traditional 3D printing technology, it can create very high-precision models, usually with higher details, smaller size and higher surface quality (Xenikakis et al., 2021). At present, technological innovation has become one of the focuses of research in the manufacturing industry. The material used is a photocurable 3D printing material, and its material selection and ratio should be selected and adjusted according to specific usage requirements (Dou et al., 2022). If used in industrial manufacturing, it should meet the requirements of low shrinkage, fast curing mechanical properties, and excellent thermal stability. If used in office or home 3D printing materials, it needs to meet the requirements of safety, non-toxic, and harmless (Luo et al., 2021). In the future, the continued development of photocuring 3D printing technology will bring new opportunities and possibilities. With the increasingly widespread application of photocuring 3D printing technology, research on related materials is also rapidly advancing.

In the field of 3D printing, inorganic organic nanocomposites have been developed to meet different needs, utilising their comprehensive properties to compensate for the defects of single component materials (Yap et al., 2021). From the perspective of rapid technological development, 3D printing technology has been highly anticipated since its inception. Its advantages of speed, efficiency, and high precision have always attracted people to explore (Bona et al., 2021). Subsequently, there is a richer and more diverse demand for raw materials, and inorganic organic nanocomposites provide researchers with more choices due to their adjustable structure and performance (Wang et al., 2021).

Therefore, developing high-performance inorganic organic nanocomposites has important practical significance for the development of 3D printing technology. Based on a brief introduction of 3D printing technology, Yang et al. (2021) emphasised the basic principles and characteristics commonly used in thermosetting and thermoplastic polymer 3D printing technology; focus on analysing the application of two different 3D printing technologies in the field of polymer nanocomposites, summarise the performance characteristics and application scope of 3D printed polymer nanocomposites, in order to lay the foundation for the widespread application of 3D printed nanocomposites. Li et al. (2022) summarised the research progress on the mechanical properties of short fibre/ continuous fibre reinforced polymer matrix composites and fibre reinforced cement-based composites both domestically and internationally in recent years from three aspects: printing methods, mechanical properties, and influencing factors. The aim was to demonstrate the types of moulding methods currently used for 3D printing fibre reinforced composites, the level of mechanical properties that can be achieved, and the influencing factors of mechanical properties, Provide reference for achieving mechanical high-performance of 3D printed fibre reinforced composite materials.

On the basis of the above research, in order to further improve the mechanical properties of UV cured 3D printing materials after curing, this article conducted a study on the mechanical properties of photocurable 3D nanofibre printing materials. By preparing THBP modified nano TiO_2, EA was used as a prepolymer, DPGDA was used as a monomer, and lithium phenyl-2,4,6-trimethylbenzene phosphonate was used as a photoinitiator. The photocurable 3D printing materials were prepared by adding THBP modified nano TiO_2 with different ratios, and analyse and studied accordingly of the materials prepared by adding THBP modified nano TiO_2 with different proportions of self synthesised THBP, in order to achieve research on strengthening and toughening modification, and to improve their mechanical properties. This can provide important reference for material design for different application scenarios, making it widely applicable.

2 Experimental analysis

2.1 Materials

The main drugs used for preparing UV curable 3D printing materials are shown in Table 1.

2.2 Instruments and equipment

The main experimental instruments used for preparing photocurable 3D printing materials are shown in Table 2.

Next, on the basis of the above raw materials and instruments, to complete the preparation of test materials. Corresponding instruments were used to conduct infrared spectrum analysis, volume shrinkage test, surface tension test, viscosity test, photocuring speed test, curing degree test, tensile strength test, impact strength test and thermal stability analysis of the prepared test materials. The results were analysed to complete the experimental study on the mechanical properties of the photocuring 3D nanofibre printing materials.

Table 1 Experimental drugs, specifications, and manufacturers

Name	*Specifications*	*Manufacturer*
KH570	AR	Shanghai McLean Biochemical Technology Co., Ltd
Nanometre TiO_2	AR	Nanjing Chemical Reagent Co., Ltd
Methylbenzene	AR	Shandong Weiming Chemical Co., Ltd
Acetic acid	AR	Shanghai Bailingwei Technology Co., Ltd
Ethanol absolute	AR	Zhejiang Tengyu Chemical Co., Ltd
Photoinitiator 819	AR	Guangchuan Electronic Materials Co., Ltd
Ethyl acetate	AR	Shanghai McLean Biochemical Reagent Co., Ltd
Epoxy acrylate	HS9103	Guangdong Tianyi Chemical Materials Co., Ltd
Oxybis (methyl-2,1-ethanediyl) diacrylate	AgiSynTM2833	Royal DSM Group
Leveling Agent 331	BYK331	Germany BYX Company
Defoamer	ST108	Dow Corning, USA

Table 2 Experimental instruments

Name	*Instrument model*	*Manufacturer*
Magnetic heating stirrer	DF-101S	Nanjing Simpson Instrument Equipment Co., Ltd
Electronic balance	JA2003N	Shanghai Precision Scientific Instrument Co., Ltd
DHG series heating and drying oven	DHG-9426	Nanjing Huanke Testing Equipment Co., Ltd
Tabletop centrifuge	LX-800	Jintan Ronghua Instrument Manufacturing Company
Vacuum oven	DZF-6050	Track and Field City Huaxing Scientific Instrument Factory
Infrared spectrometer	Nicolet Nexus 670	Nicolet Company in the USA
Simultaneous thermal analyser	TA	German Company NETZSCH
UV curing machine	RK-400/2	Lixin Technology Co., Ltd
LCD curing 3D printer	X8.9	Nanjing Guangzhu Intelligent Co., Ltd
Digital viscometer	NDJ-5S	Shanghai Shunyu Hengping Scientific Instrument Co., Ltd
Electronic densitometer	TW-120S	Shanghai Fangrui Instrument Co., Ltd
Surface tension meter	ZF2-100	Shanghai Zhongchen Technology Equipment Co., Ltd
Scanning electron microscope	S-3400N	Company Hitachi in Japan
Universal mechanical performance testing machine	CMT5105	Shenzhen Xinsansi Material Testing Co., Ltd
Pendulum impact testing machine	XJ-300A	Wuzhong Material Testing Machine Co., Ltd

2.3 Material preparation

2.3.1 KH570 nanometers TiO_2

Take an appropriate amount of nano TiO_2 and place it in DHG series heating and drying oven. Dry it at 100°C for 12 h and take it out for later use. Add 150 ml of methylbenzene to a 500 ml four port flask equipped with a thermometer, magnet and oil-water separator, accurately weigh 10 g of vacuum dried nano TiO_2, stir in methylbenzene, and sonicate for 30 min. Afterwards, a mixed solution consisting of 10 ml deionised water, 10 ml ethanol absolute, 2 ml formic acid, and 2 g KH570 was added to a four necked flask, heated to reflux temperature, and stirred for 4 h (Wang et al., 2020). Centrifuge the stirred product using tabletop centrifugation, and then wash it four times with diluted water. Place it in a vacuum oven for 12 h to obtain KH570 modified nano TiO_2, denoted as KH570-TiO_2.

2.3.2 Surface grafting of tert butyl hydrogen peroxide THBP onto nano TiO_2

Weigh 1 g of the above modified nano TiO_2, 30 g of THBP, 0.1 g of photoinitiator 819, and 50 ml of ethanol solution, and add them to a three necked flask with a stirrer thermometer. Fully stir and mix the reactants at ambient temperature, and expose the reaction vessel to ultraviolet radiation with a main wavelength of 365 nm for 10 consecutive hours (Asano et al., 2021). Next, the mixture was subjected to a 12 hour extraction process in toluene to eliminate the unreacted portion and residual THBP on the surface of nano TiO_2. The resulting product was dried at 90°C for 12 h to obtain THBP modified nano TiO_2, denoted as THBP-TiO_2.

2.3.3 Preparation of UV cured 3D nanofibre printing materials

1 Bisphenol A type epoxy acrylate (EA) and dipropylene glycol diacrylate (DPGDA) with a mass ratio of 1:1 were added into the beek, and the temperature was set to 57°C in a magnetic heating agitator. The stirring lasted for 30 min at the rotation speed of 10 rad/s, and finally the transparent solution was obtained (Liu et al., 2021).

2 Next, use electronic balance to weigh 125 g of THBP and a certain amount of THBP-TiO_2, and then mix them into the transparent solution mentioned above. Stir for 30 min at a speed of 10 rad/s at 57°C until THBP is completely dissolved and THBP-TiO_2 is evenly dispersed.

3 Finally, 1 wt/% photoinitiator 819 should be taken under the condition of avoiding light, mixed with the additive with a mixing ratio of 1:1 between levelling agent and defoamator, and poured into the solution obtained by stirring. The stirring operation lasted for 30 min at 25°C was carried out to obtain THBP-TiO_2 modified photocuring 3D printing materials. According to the above operations, in order to ensure the convenience of the experiment, improve the efficiency and accuracy of the experiment, the influence trend of THBP-TiO_2 content on the performance of the photocured 3D nanofibre printing material was observed, and then the optimal content range was determined. This time, different THBP-TiO_2 contents such as 0, 1, 3, 5 and 7 wt/% were selected to prepare photocurable 3D printing materials to explore its influence on material properties. Meanwhile, a certain content range was also covered to obtain more comprehensive experimental data. The available formula of each sample is shown in Table 3.

Table 3 Specific formula of UV cured 3D nanofibre printing materials (wt/%)

Sample group	*EA*	*DPDGA*	*THBP*	*THBP-TiO₂*	*819*	*Auxiliary*
#1	40	40	25	0	1	1
#2	40	40	25	1	1	1
#3	40	40	25	3	1	1
#4	40	40	25	5	1	1
#5	40	40	25	7	1	1

Take 200 g of different formulations of UV curable 3D nanofibre printing materials and add them to the LCD UV curable 3D printer. Establish 50 μm print layer thickness, and use a 15 s exposure duration for each individual layer during the printing process. Through UV curing at the bottom of the LCD screen, the UV curing material is cured at a rate of 50 μm the layer thickness of is solidified and overlaid to form. Finally, tensile test strips in accordance with GB/T 1042-1992 and GB/T 1043.1-2008 will be produced. Next, conduct the following tests on the prepared materials and test samples.

2.4 Testing and characterisation

Adjust the test on the required instruments before the test starts to avoid error in the results. In addition, external factors such as temperature and humidity in the laboratory environment will also affect the results of experimental tests, so it is necessary to control the temperature in the laboratory between 20–25°C and the relative humidity in the laboratory between 40–60% and strictly in accordance with the corresponding operation of the test.

2.4.1 Infrared spectra analysis (FTIR)

Using infrared spectrometer for testing, firstly, vacuum oven was used to dry potassium bromide KBr, and a certain amount was weighed for grinding. After grinding, the material was pressed into thin sheets. Then, the uncured material was evenly applied onto the KBr sheet and tested in an Infrared spectrophotometer to obtain the projected infrared spectroscopy of the photo cured material to be cured; place the cured material in an infrared spectrometer for drying treatment, then weigh an appropriate amount of KBr powder and mix it to grind, press it into thin sheets, and test it with an infrared spectrometer to obtain the transmission infrared spectroscopy of the cured sample (Prem, 2020).

2.4.2 Volume shrinkage

Test the volume shrinkage of THBP-TiO_2 materials with different content by TW-120S electron density meter (Li, 2021). The calculation formula is shown in equation (1).

$$\Delta = \frac{\rho_2 - \rho_1}{\rho_2} \tag{1}$$

In the equation, ρ_1 and B ρ_2 is the density of the material before and after curing at 25°C.

2.4.3 Surface tension

According to GB/T 22237-2008, the ZF2-100 fully automatic surface tension meter was used to measure the surface tension of photo cured resin cured with different contents of THBP-TiO_2 at 25°C (Jenei et al., 2021).

2.4.4 Viscosity

By using NDJ-5S digital viscometer and according to GB/T22235-2008, the viscosity of UV cured materials with different contents of THBP-TiO_2 added before curing was tested at 25°C (Tayeb et al., 2022).

2.4.5 UV curing speed

Measure the UV curing rate of the five groups of materials in Table 3 using a UV curing machine, and the obtained values are judged to be fully cured according to the GB1728-79 standard. By continuously adjusting the transmission speed of the track until the one-time curing thickness is 100 μm obtain the UV curing rate of the material using the curing film (Wang, 2021).

2.4.6 Degree of cure

According to GB/T 2576-2005, UV curable 3D printing materials containing different amounts of THBP-TiO_2 are cured and ground into powder. They are weighed, and their mass is recorded as m_1. Then, they are dried for a period of 2.1 hours. Afterwards, it will be weighed and its mass recorded as m_2. Next, wrap the dried sample with dry filter paper and place it in the Soxhlet extraction device as shown in Figure 1. Using isopropyl alcohol as a solvent, extract in an oil bath at 90°C for 8 h at a siphon frequency of 10 minutes per time. Then, place the resulting sample again in a vacuum oven for 10h of drying treatment. Finally, weigh it and record its mass as m_3. The curing degree calculation formula is shown in the following equation.

$$\varphi = \frac{m_3 - m_1}{m_2 - m_1} \tag{2}$$

2.4.7 Tensile strength

Using a competency testing machine and in accordance with GB/T 1042.1-2004, perform 10 corresponding tests on the tensile strength of five specimens. Calculate the average of the results of this test to obtain the final tensile strength results of 3D printed materials (Gz et al., 2022). The calculation formula is shown in equation (3):

$$\sigma = \frac{F}{b \times h} \tag{3}$$

In the formula, σ is the tensile strength, F is the maximum load, b is the sample width, and h is the sample thickness.

Figure 1 Soxhlet extraction device diagram (see online version for colours)

2.4.8 Impact strength

According to GB/T 1043.1-2008, ten impact performance tests were conducted on the five specimens prepared using the XJ-300A pendulum impact testing machine. The average value of the test results was calculated to determine the impact strength of the final 3D printed material (Wang et al., 2022). The calculation formula is shown in Figure 4.

$$\sigma_{cN} = \frac{E_c}{b \times h} \tag{4}$$

In the formula, σ_{cN} is the impact strength, and E_c is the energy absorbed during failure.

2.4.9 Thermal stability analysis (TGA)

After curing, dry and grind the UV curable 3D printing material with different THBP additions into powder. Take 3mg of the sample and load it into the thermal gravimetric analyser crucible. Use NETZSCH to synchronously heat the thermal gravimetric analyser from room temperature to 600°C to record thermal weight loss data (Korkunova et al., 2022). Its heating rate is 10°C/min, and the nitrogen flow rate is 20 ml/min.

3 Result analysis

3.1 Infrared spectroscopy analysis before and after curing

To verify the effectiveness of the prepared material, the infrared spectrum results of the material with the addition of THBP-TiO_2 before and after UV curing were analysed.

Taking the material with the addition of 3 wt% THBP-TiO_2 as an example, the infrared spectrum results before and after curing are shown in Figure 2.

Figure 2 Infrared spectra of THBP-TiO_2 modified UV curable material (see online version for colours)

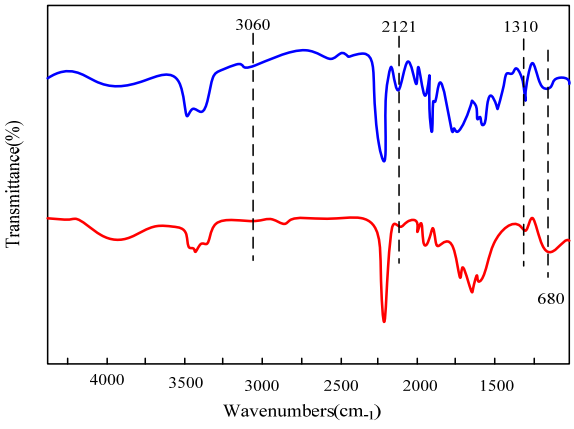

The results shown in Figure 2 show that after curing, the stretching and bending vibration peaks of $C = C$ at 1,621 cm^{-1} and 810 cm^{-1} of the THBP-TiO_2 modified photocurable material basically disappear, while the infrared characteristic peak of – SH and Ti-O at 2,560 cm^{-1} and 680 cm^{-1}, respectively. The former disappears after curing, while the latter remains almost unchanged compared to before curing. These observations indicate that the combination of ultraviolet light and photoinitiators promotes the crosslinking polymerisation of prepolymers and monomers through double bonds or thiol groups in the system, resulting in higher conversion rate. At the same time, THBP-TiO_2 also participates in the photocuring reaction through the thiol groups on the surface, connecting to the cross-linking network. This indicates that THBP-TIO_2 can participate in the curing reaction of the materials, and the addition of THBP-TiO_2 can modify the properties of photocured 3D printing materials, the prepared material has effectiveness.

3.2 Process performance analysis

3.2.1 Volume shrinkage rate

The test was carried out on the materials with different mass fractions of THBP-TiO_2, and the results can show the reliability of the material used to print the generative model, as shown in Figure 3.

According to the results obtained in Figure 3, t is evident that with the increase of THBP-TiO_2 content, the volume shrinkage of the material shows a decreasing trend. According to the above results, when the content of THBP-TiO_2 added to the material reaches 7 wt%, the volume shrinkage of the material is reduced to 4%. Due to the presence of THBP-TiO_2 as a polymer organic filler in liquid photocurable 3D printing materials, phase separation occurs during the curing process, which can offset some volume shrinkage, thus reducing in a decrease in material volume shrinkage with an increase in THBP-TiO_2 content.

Figure 3 Volume shrinkage test results

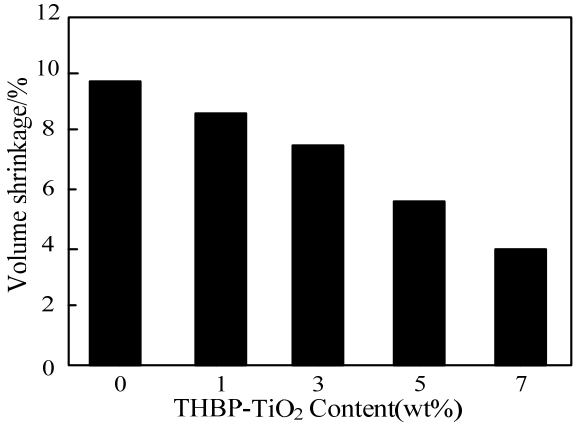

3.2.2 Viscosity

To ensure the normal operation of UV cured 3D printing, it is usually required that the viscosity of the material should not exceed 200 MPa·s. Figure 4 shows the viscosity of the viscosity of materials with different mass fractions of THBP-TiO_2 added at 25°C.

Figure 4 Viscosity analysis

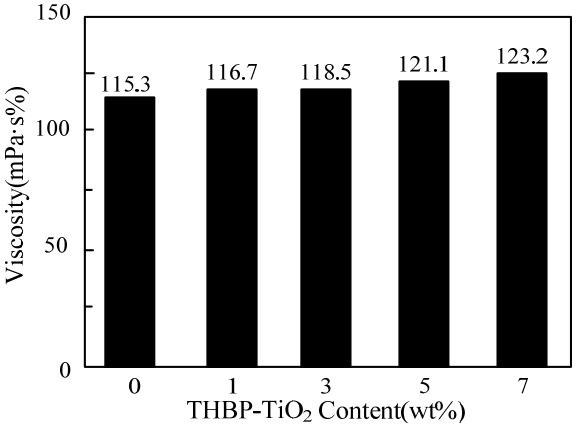

As shown in the figure, by continuously increasing the content of THBP-TiO_2, the viscosity of the material also shows a small increasing trend. When the THBP-TiO_2 content is 5 wt%, the viscosity of the material increases by about 5.8 MPa·s compared to the unmodified one. Due to the presence of THBP-TiO_2 in the form of rigid particles in liquid photocurable 3D printing materials, its hindrance to the movement of pre-polymers and monomer molecular chains is the main reason for the increase in viscosity of photocurable 3D printing materials.

3.2.3 Surface tension

The surface results can clearly demonstrate the spreading ability of the materials. Figure 5 shows the surface tension of the materials with different mass fractions of THBP-TiO_2 added at 25°C.

Figure 5 Surface tension analysis

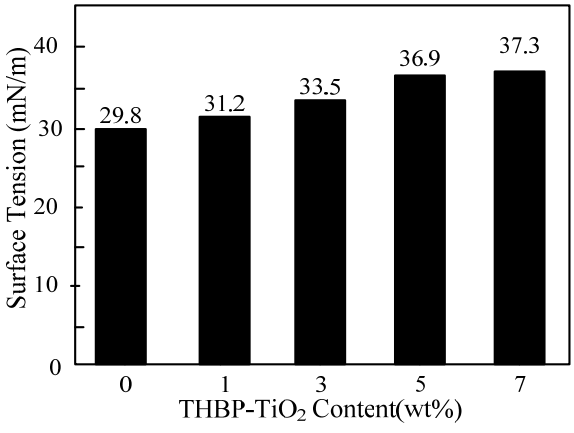

From the results obtained in Figure 5, the surface tension of the UV cured 3D printing material is positively proportional to the amount of THBP-TiO_2 added. An increase in the amount of THBP-TiO_2 can improve the surface tension of the material to a certain extent. Compared to the increase in viscosity, the increase in surface tension of the material is greater. When the THBP-TiO_2 content is 5 wt%, the surface tension of the material increases by about 7.1 mN/m. This is mainly due to the existence of THBP-TiO_2 in the form of high surface energy nanoparticles in the materials, and the introduction of the interaction between solid and liquid phases enhances the surface tension of the system.

3.2.4 UV curing speed

The UV curing speed of UV cured 3D printing materials directly determines the moulding speed and production cost of UV cured 3D printing. The results of the UV curing speed of materials prepared by adding various contents of THBP-TiO_2 are shown in Figure 6.

As shown in the figure, the UV curing rate of the material is inversely proportional to the amount of THBP-TiO_2 added. The increasing amount of THBP-TiO_2 can lead to a certain downward trend in the UV curing rate of the material. The main reasons include two points: on the one hand, the addition of TEBP-TiO_2 leads to a continuous increase in the viscosity of the system, hindering the movement of polymer and monomer molecular chains, and reducing the probability of collision between free radicals and active groups; on the other hand, THBP-TiO_2 exists in the form of nano particles, which can reflect, refract and absorb UV light to a certain extent, reducing the rate of the decomposition of photoinitiators to produce primary free radicals.

Figure 6 Analysis of UV curing speed

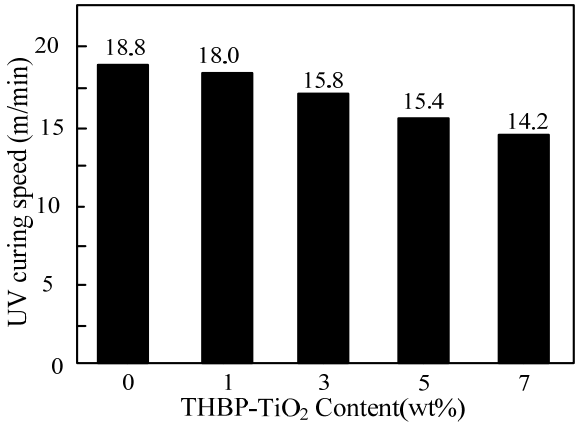

3.2.5 Curing degree

The degree of curing reflects the degree to which each component in the material participates in the UV curing reaction, which usually directly affects the mechanical properties of the material. Figure 7 reflects the effect of THBP-TiO_2 content on the degree of curing of the material.

Figure 7 Analysis of curing degree

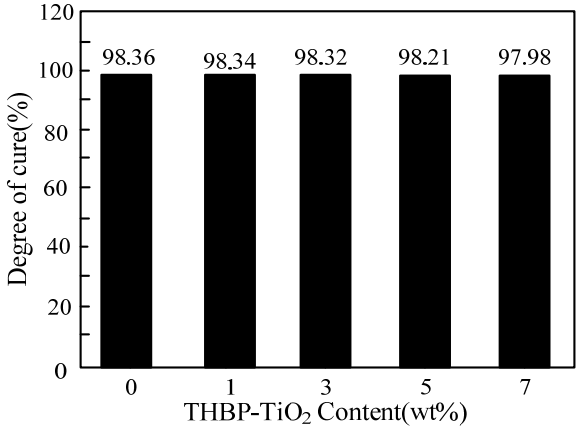

This figure indicates that when THBP-TiO_2 is added in an amount below 3 wt%, there is no significant change in the curing degree of the material. This indicates that THBP-TiO_2 is uniformly distributed in the cross-linking network and participates in the UV curing reaction in a highly effective manner, thereby minimising the impact on the overall curing degree. Further increase in the content of THBP-TiO_2 will affect the curing degree of the material, resulting in a slight downward trend. The reason for this phenomenon is that when the content of THBP-TiO_2 reaches a certain value, excessive surface energy will cause it to aggregate and distribute in the form of larger particles in the material. The

spatial hindrance effect generated will hinder the progress of the UV curing reaction, thereby reducing the degree of curing of the system.

3.3 Mechanical properties

3.3.1 Tensile strength

By testing the tensile strength of samples prepared after curing of five different THBP-TiO_2 contents of UV cured 3D printing materials, the mechanical properties of the materials were reflected. The tensile strength results are shown in Figure 8.

Figure 8 Tensile strength analysis

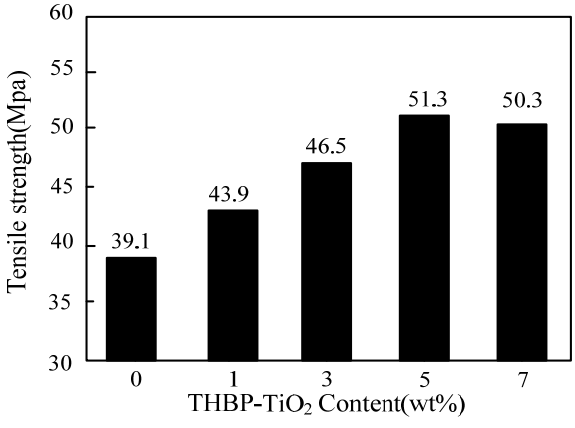

The figure indicates that adding THBP-TiO_2 to the material initially enhances its tensile strength, but when the THBP-TiO_2 content exceeds a certain value, the tensile strength begins to decrease. This is mainly because when the content of THBP-TiO_2 reaches a certain value, excessive surface energy will cause it to aggregate and distribute in the form of larger particles in the UV cured 3D printing material. The spatial hindrance effect generated by it will hinder the progress of the UV curing reaction, thereby reducing the tensile strength. When the addition amount of THBP-TiO_2 exceeds 5 wt%, its tensile strength shows a decreasing trend. Therefore, when the addition amount of THBP-TiO_2 is 5 wt%, the tensile strength of the sample can reach a maximum of 51.3 MPa.

3.3.2 Impact strength

By testing the impact strength of samples prepared after curing of five different THBP-TiO_2 contents of UV cured 3D printing materials, the mechanical properties of the materials were reflected. The impact strength results are shown in Figure 9.

As shown in the figure, as the THBP-TiO_2 content gradually increases, the impact strength of the material initially continuously increases. However, as the THBP-TiO_2 content exceeds a certain amount, the impact strength begins to decrease, similar to the tensile strength. The reason is the same as above. When the addition content of THBP-TiO_2 is 5 wt%, the impact strength can reach its maximum of 22.1 KJ/m^2.

Figure 9 Tensile strength analysis

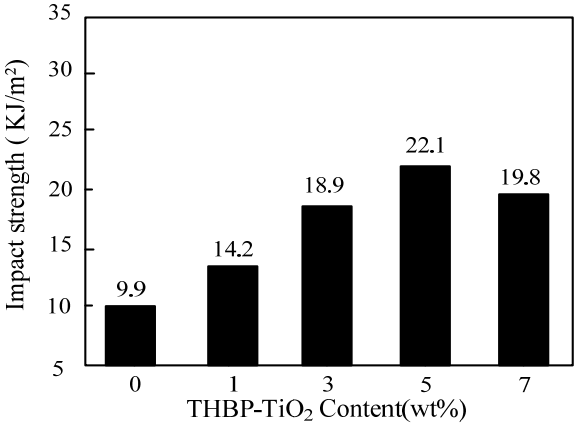

3.4 Thermal stability analysis

This test can reflect the stability of the materials under high temperature environments. The effects of different THBP-TiO_2 contents on the thermal stability of the materials are shown in Figure 10 and Table 4, respectively.

Figure 10 Thermogravimetric analysis TGA curves of THBP-TiO_2 materials with different contents (see online version for colours)

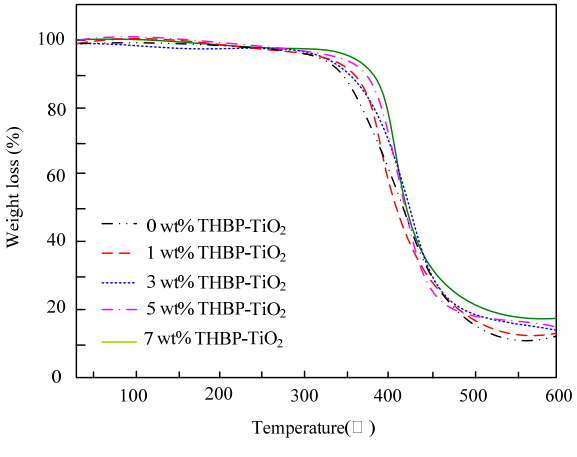

From Figure 10, the material does not contain water or organic solvents, as no significant weight loss was observed below 150°C; between 340°C and 460°C, the sample exhibited significant thermal weight loss, mainly due to the thermal decomposition of molecular chains in the polymer network. By detecting the residual mass of thermal decomposition of different samples at 600°C, it was found that the residual mass of high-temperature thermal decomposition of the material increases with the increase of THBP-TiO_2 content, which adheres to the surface of the polymer matrix and further hinders the thermal

decomposition of the polymer, thereby improving the thermal stability of the material and enhancing it.

Table 4 Thermogravimetric analysis TGA data of THBP-TiO_2 materials with different contents

THBP-TiO_2 content (wt%)	$T_{5\%}$	$T_{50\%}$	T_{max}
0	324	426	525
1	343	428	529
3	351	430	536
5	362	432	542
7	378	434	553

The data in Table 4 shows that the initial decomposition temperature (5% mass loss) of the UV cured 3D printing material increases with the increase of THBP-TiO_2 content. This can be attributed to THBP-TiO_2 being the cross-linking centre in the cross-linking network, resulting in improved interactions between polymer molecular chains and a decrease in the proportion of flexible segments. Regarding the median decomposition temperature (50% mass loss), it was observed that adding materials with higher THBP-TiO_2 content slightly increased the temperature required to decompose 50% mass, indicating a decrease in the thermal decomposition rate of the material. It is due to the steric hindrance effect of THBP-TiO_2, which limits the thermal motion of polymer molecular chains. In addition, after the surface hyper-branched structure is destroyed, the remaining nano TiO_2 adheres to the polymer matrix, hindering thermal diffusion and transfer. The inspection results of the maximum thermal decomposition temperature of various samples indicate that the continuous addition of THBP-TiO_2 leads to a continuous increase in the maximum thermal decomposition temperature of the material, indicating an improvement in its thermal stability.

4 Conclusions

Firstly, it was demonstrated that THBP-TiO_2 can participate in the curing reaction of UV curable 3D printing materials, and it was determined that the addition of THBP-TiO_2 can modify the properties of UV curable 3D printing materials, and the prepared materials have effectiveness. Subsequently, the effects of the amount of TEBP TiO_2 added on the material's processing properties, mechanical properties, and thermal stability were studied, as well as its dispersibility and strengthening and toughening mechanism in UV cured 3D printing materials. The main research conclusions are as follows:

Increasing the content of THBP-TiO_2 can reduce the volume shrinkage of the UV curable 3D printing material, and the reliability of the UV curable 3D printing generative model can be effectively improved. The viscosity and surface tension of the material gradually increase, and the UV curable speed and curing degree show a downward trend. In terms of mechanical properties, when the TEBP-TiO_2 content is 5 wt%, the tensile strength and impact strength of the samples prepared after UV curing reach 51.3 MPa and 22.1 KJ/m^2, respectively. After the maximum value exceeds 5 wt%, its tensile strength and impact strength begin to show a downward trend. In terms of stability, the thermogravimetric analysis results show that as the THBP-TiO_2 content gradually

increases, the initial and maximum decomposition temperatures of the material increase. When the THBP-TiO_2 content is 7 wt%, the initial and maximum decomposition temperatures of the UV cured 3D printing material increase to 378°C and 553°C, respectively. The residual mass of thermal decomposition increases, and the thermal stability is improved. Through the results of the above research, the research on strengthening and toughening modification of photocurable 3D nanofibre printing materials is achieved, with the aim of improving their mechanical properties. This provides important reference for material design for different application scenarios, and will be widely applied in many fields in the future, such as biomedicine, electronic industry, environmental protection, etc. which will have a positive impact on human life and social development.

Acknowledgements

This work was supported by Project of Hunan Provincial Social Science Achievement Review Committee under Grant No. XSP22YBC062.

References

Asano, A., Nakagawa, M., Miyajima, C. et al. (2021) 'Effect of the powerful plasticity of the tert-butyl side chain on the conformational equilibrium of ascidiacyclamides', *Journal of Peptide Science*, Vol. 27, No. 12, pp.1–9.

Bona, A.D., Cantelli, V., Britto, V.T. et al. (2021) '3D printing restorative materials using a stereolithographic technique: a systematic review', *Dental Materials*, Vol. 37, No. 2, pp.336–350.

Dou, R., Tang, W., Hu, K. et al. (2022) 'Ceramic paste for space stereolithography 3D printing technology in microgravity environment', *Journal of the European Ceramic Society*, Vol. 42, No. 9, pp.3968–3975.

Gz, A., Qw, A., Yn, A. et al. (2022) 'A systematic investigation on the minimum tensile strengths and size effects of 3D printing polymers', *Polymer Testing*, Vol. 117, No. 8, pp.24–28.

Gzab, C., Bzab, C., Xwab, C. et al. (2022) 'Design, manufacturing and properties of controllable porosity of ceramic filters based on SLA-3D printing technology', *Ceramics International*, Vol. 49, No. 1, pp.1009–1019.

Jenei, M., Akkermans, R., Robertson, S. et al. (2021) 'Molecular simulation of thermoset curing: application to 3D printing materials', *Molecular Simulation*, Vol. 47, No. 9, pp.575–585.

Korkunova, O.S., Kholkhoev, B.C. and Burdukovskii, V.F. (2022) 'Photosensitive thiolene composition for DLP 3D printing of thermally stable polymer materials', *Mendeleev Communications*, Vol. 32, No. 2, pp.231–233.

Li, A. (2021) 'Study on curing shrinkage and mechanism of DHOM-modified epoxy-acrylate-based UV-curing 3D printing materials', *Journal of Applied Polymer Science*, Vol. 138, No. 8, pp.4–9.

Li, Y., Long, Y., Hao, L.C. et al. (2022) 'Research progress on mechanical properties of 3D printed fiber reinforced composite materials', *Mechanics Quarterly*, Vol. 43, No. 4, pp.731–750.

Liu, S., Graff, B., Xiao, P. et al. (2021) 'Nitro-carbazole based oxime esters as dual photo/thermal initiators for 3D printing and composite preparation', *Macromolecular Rapid Communications*, Vol. 42, No. 15, pp.1–6.

Liu, Y., Lu, G., Lin, Y. et al. (2022) 'Enhanced thermal conductivity of epoxy acrylate/h-BN and AlN composites by photo-curing 3D printing technology', *Journal of Applied Polymer Science*, Vol. 139, No. 29, pp.1–12.

Luo, B., Shen, Z., Cai, Z. et al. (2021) 'Layered nanosheets: superhierarchical inorganic/organic nanocomposites exhibiting simultaneous ultrahigh dielectric energy density and high efficiency (Adv. Funct. Mater. 8/2021)', *Advanced Functional Materials*, Vol. 31, No. 8, pp.21–25.

Prem, D. (2020) 'Infrared spectral analysis of low concentration magnetoactive polymers', *Journal of Applied Polymer Science*, Vol. 137, No. 7, pp.31–36.

Tayeb, A., Cam, J. and Loez, B. (2020) '3D printing of soft thermoplastic elastomers: effect of the deposit angle on mechanical and thermo-mechanical properties', *Mechanics of Materials*, Vol. 165, No. 5, pp.1–11.

Wang, W., Sun, S. and Hu, S. (2022) 'Unprecedented strength polysiloxane-based polyurethane for 3D printing and shape memory', *ACS Applied Materials & Interfaces*, Vol. 14, No. 2, pp.3324–3333.

Wang, Y. (2021) 'Polyethylene glycol modified epoxy acrylate UV curable 3D printing materials', *Journal of Applied Polymer Science*, Vol. 138, No. 13, pp.9–14.

Wang, Y., Li, H., Wang, D. et al. (2021) 'Inorganic-organic nanocomposites based on aggregation-induced emission luminogens', *Advanced Functional Materials*, Vol. 31, No. 7, pp.1–18.

Wang, Z., Yuan, L., Liang, G. et al. (2020) 'Mechanically durable and self-healing super-hydrophobic coating with hierarchically structured KH570 modified SiO_2-decorated aligned carbon nanotube bundles', *Chemical Engineering Journal*, Vol. 408, No. 4, pp.1–15.

Xenikakis, I.T., Tzimtzimis, K. et al. (2021) 'Fabrication of hollow microneedles using liquid crystal display (LCD) vat polymerization 3D printing technology for transdermal macromolecular delivery', *International Journal of Pharmaceutics*, Vol. 597, No. 1, pp.3–6.

Yang, Z.Z., Kong, Z.W., Wu, G.M. et al. (2021) 'Research progress in 3D printed polymer nanocomposites', *Materials Introduction*, Vol. 35, No. 13, pp.13177–13185.

Yap, X.Y.S., Goh, I. et al. (2021) 'Mechanical properties and failure behaviour of architected alumina microlattices fabricated by stereolithography 3D printing', *International Journal of Mechanical Sciences*, Vol. 196, No. 1, pp.245–251.

Yong, Z., Lsab, C., Hyab, C. et al. (2022) 'Fabrication of alumina ceramics with functional gradient structures by digital light processing 3D printing technology – ScienceDirect', *Ceramics International*, Vol. 48, No. 8, pp.10613–10619.